DOI:
10.1136/thoraxjnl-2017-211073

Document Version
Other version

The skeletal muscle metabolic phenotype in early critical illness: ONLINE SUPPLEMENT

eMethods

1.Western blotting and Luminex platform

Primary antibody	Supplier	Product code	Monoclonal
P-AMPK (thr172)	Cell Signalling	#2535	Y
T-AMPK	Abcam	Ab80039	Y
Fatty Acid Oxidation Panel	Merck Millipore	HFA02MAG-11K	N/A
Mitochondrial Respiratory Chain Panel	Merck Millipore	HOXPSMAG-16k	N/A

Table S1: Antibodies used for Western Blotting and Reagents for Luminex Platform. AMPK=Adenosine Monophosphate Kinase

2. Quantitative Polymerase Chain Reaction measurements

Primer Name	Primer Sequence	NCBI Accession number
hsaDNM1L_001	(f)gtggaagcagaagaatggggta (b) tacaggcaccttggtcattcc	NM_012062, NM_012063, NM_005690
hsaPPARGC1A_001	(f) tcgcagtcacaacacttacaag (b) ggttatcttggttggctttatgagg	NM_013261
Hsa_PPARGC1B_001	(f) gaaataggagaggcgagaagtacg (b) gcctcttctgaattggaatcgtag	NM_133263, NM_001172698.1 NM_001172699.1
HsaPPRC1_001	(f) atcagtgagattggaattgaggca (b) tcttctcctggggaatgtcaac	NM_015062

Table S2: Primers used for Quantitative Polymerase Chain Reaction

2.1 Mitochondrial copy number assay

Reactions were run in a Rotor-Gene with standards at 10^8-10^2 copies/rxn for mitochondrial DNA and 10^7-10^1 copies/rxn for a single copy nuclear DNA gene, B2M. For the mitochondrial assay, primers targeted a unique region of the mitochondrial genome that is not replicated in the nuclear genome[1]. The nuclear DNA assay was designed and validated by qStandard (London, UK).

3. Untargetted metabolic profiling with lipid optimisation: Global untargeted LC-Mass Spectroscopy Methods for Muscle: Reverse Phase and HILIC

Sample Preparation Organic

Samples were prepared for liquid chromatography mass spectrometry (LCMS) as per venous tissue described by Anwar et al[2]. Prior to use, the original samples were

randomized using excel (RAND) command and numbered sequentially. These samples were thawed (11 samples at a time), weighed and placed in pre-labelled Eppendorfs numbered 1-105, plus 20 blanks. A 12th sample tube was to prepare a blank of solvent.

1ml of refrigerated Methyl *tert*-butyl ether / Methanol (MTBE/MeOH) solution was added to each of the 11 sample-containing Eppendorfs and to the 12th (blank) tube. 1 capful of Zirconium beads (1mm) was added to each sample, and the caps securely closed. The samples were then loaded into a *Precellys* Bead-Beater (www.strettonscientific.co.uk) (maximum sample capacity of 12) for 40 seconds Following this samples were cooled on dry ice for 5 minutes before repeat bead beating,

After two cycles of bead-beating, the cooled samples were centrifuged at 4°C for 20 minutes, the centrifuge being fast-cooled before use.

750µl of supernatant was then pipetted into a fresh pre-labelled Eppendorf (identifying sample no, and extraction type: organic).

Original sample tubes were kept on ice post-removal of the first aliquot of supernatant. The supernatant itself is metabolite stable and may be kept at room temperature.

A further 1ml of MTBE/MeOH solvent was added to each cooled original sample tube. Bead-beating was performed twice as before with the sample cooled for 5 minutes on dry ice in between beat-beating repetitions. The samples were then centrifuged as before. 750µl of the resulting supernatant was aliquoted into the Eppendorfs already containing 750 µl. This step was repeated to increase potential metabolite yield, as sample size was small. The residual solvent remaining in the each of original Eppendorfs was then removed and aliquoted into a glass tube. This was to avoid contaminating the aqueous extraction step, as MTBE is not water miscible. The original samples were cooled on dry ice.

The 12 samples were uncapped and the solvent allowed to evaporate in a fume-hood overnight.

After overnight solvent evaporation, extracts were stored at -80°C for reconstitution prior to use and transferred to total recovery glass LCMS grade vials. 50 µl from each vial was used to make a quality control (QC).

Reconstitution of frozen extracts

<u>Reconstitution of Organic Samples for LCMS</u>

Dried organic extracts were reconstituted in 250µl isoprenol/acetonitrilewater (ISP/ACN/H_20) (2:1:1). Samples were vortexed for 1 minute then sonicated for 5 minutes. They were then vortexed for 1 further minute. This was followed by centrifugation at 4°C for 8 minutes. Samples were then transferred to total recovery glass LCMS grade vials. 50 µl from each vial was used to make a QC.

UPLC-MS experimental parameters

Chromatographic conditions were as previously described[3] and derived from previous Waters applications (www.waters.com). Mobile phase A consisted of ACN/water (60:40) and mobile phase B ISP/ACN (90:10). In both solutions ammonium formate was diluted to 10 mM and formic acid to 0.1%. The elution gradient was set as follows: 60−57% A (0.0−2.0 min), 57−50% A (2.0−2.1 min; curve 1), 50−46% A (2.1−12.0 min), 46−30% A (12.0−12.1 min; curve 1), 30−1% A (12.1−18 min), 1−60% A (18.0−18.1 min), 60% A (18.1− 20.0 min). The temperature was maintained at 55°C on a Waters Acquity UPLC HSS CSH column (1.7 µm, 2.1 × 100 mm) during chromatography. Tandem time of flight (TOF) mass spectrometry (MS) was performed using an electrospray injection (ESI) ionisation operating in both positive and negative modes. ESI conditions were source temperature 120°C, desolvation temperature 400°C, cone gas flow 25L/h, desolvation gas 800L/h, capillary voltage for ESI- 2500V, for ESI +ve 3000 V, cone voltage 25 V for ESI -ve and 30V for ESI +ve. Each injection was of 5µL for +ve ESI and 15µL for –ve ESI modes. At the start of acquisition, ten conditioning QC injections were performed and after every 10th subsequent injection. Data were collected in centroid mode. Regular injections of leucine enkephalin (555.2692 Da calculated monoisotopic molecular weight, 200pg/uL in acetonitrile:water 50:50) were performed to ensure optimum mass accuracy with an analyte-to-reference scan ratio of 10:1. Instrument calibration was with sodium formate (10ng/uL in 90:10 propan-2-ol:water) solution prior to each ESI mode.

4. Adipokinin assays

Adipokine	Product Code
Ghrelin	EZGRT-89K
Leptin	EZHL-80SK
Adiponectin	EZHADP-61K
Resistin	EZHR-95K

Table S3: Enzyme-linked Immunosorbent Assay (ELISA) product codes. (Merck MIL-lipore, UK)

5. Bioenergetic data

Muscle total creatine, phosphcreatine and adenosine triphosphate contents were determined in a control population and compared to that of the critically ill cohort.

Resting muscle ATP content may be reduced in patients with chronic diseases such as Chronic Obstructive Pulmonary Disease[4 5]. Prior to critical illness, 46% of our patient cohort had suffered a chronic disease state. The control subject cohort was thus selected to contain a similar proportion (48%) of previously chronically unwell.
The young healthy volunteer muscle ATP, phosphocreatine and free creatine control data represent unpublished historical archived data from baseline muscle biopsy samples obtained from experiments published in 2011[6 7]. This study received local ethical approval and all volunteers provided informed consent for skeletal muscle biopsies of vastus lateralis that included the determination of muscle metabolite concentrations.
The older control muscle ATP, phosphocreatine and free creatine data are also unpublished historical archived data and were determined in muscle biopsy samples from a healthy age matched volunteer cohort in addition to the COPD cohort. Again, local ethical approval was obtained and all volunteers provided informed consent for skeletal muscle biopsies of vastus lateralis that included the determination of muscle metabolite concentrations.
All muscle metabolite data generated at the University of Nottingham as part of PhD research programmes and collaborations between the Universities of Leicester (old controls; Research Ethics Committee number 04/Q2502/43) and Nottingham (young controls; Research Ethics Committee number G/2/2005). These are unpublished historical archived data and the aims of the original studies were in no way connected to the present study.
The first day of ICU admission does not necessarily reflect the first day of critical illness, and it is thus possible that muscle ATP content had declined during antecedent decline in clinical state. However, whilst unable to quantify physiological derangement prior to admission, the median time from hospital to ICU admission was only 24 hours. In addition 16/34 patients suffered major trauma or an intracranial bleed and were not exposed to antecedent decline.

To confirm the validity of our cohort, we therefore (as performed for loss of muscle mass previously[8]) analysed the cohort for differences related to pre-ICU admission length of stay, or to potential antecedent decline. Analysis was also performed by presence/absence of prior chronic disease. The impact of antecedent chronic disease on trajectory of muscle ATP decline during critical illness was also examined.

6. Network analysis

Data were loaded into R 3.2. Pairwise correlation was calculated for all variables. These pairwise correlations were converted to a weighted, directed network where each node represented a variable, the direction of the edge reflected the direction of the correlation and the weight of each edge was the absolute of the correlation coefficient. Edges with a weight < .4 were removed.
This network was imported into Cytoscape 3.4.0 for visualisation and clustering. Data were visualised using a force-directed layout, with edges coloured by direction and with the width of the line determined by the weight of the edge (the correlation coefficient). Finally, variables were clustered in Cytoscape using MCclust.

R Code used:

```
library(magrittr)

zudin.all.data <- read.csv("R:/Lindsay/KCL/Zudin 2015/lindsay modelling 180716.csv", header=TRUE,
na.strings=c("/", "n/a"), stringsAsFactors=FALSE)
zudin.all.data <- zudin.all.data[-34,]
rownames(zudin.all.data) = zudin.all.data$UIN
zudin.all.data <- zudin.all.data[,-1]

zudin.numeric = unlist(zudin.all.data) %>% as.numeric %>% matrix(nrow = 33, ncol = 55)
colnames(zudin.numeric) = names(zudin.all.data)
rownames(zudin.numeric) = rownames(zudin.all.data)

# export to Cytoscape
thresh = .4
temp1 <- cor(zudin.numeric, zudin.numeric, use = 'pairwise.complete.obs')
hist(temp1, 50)

exportNetworkToCytoscape(temp1,
                edgeFile = "adjCor.network.DIRECTED.xxxxxx.txt",
                weighted = T,
                nodeNames = colnames(zudin.numeric),
                threshold = thresh)
```

eResults

1. Consort Flowchart

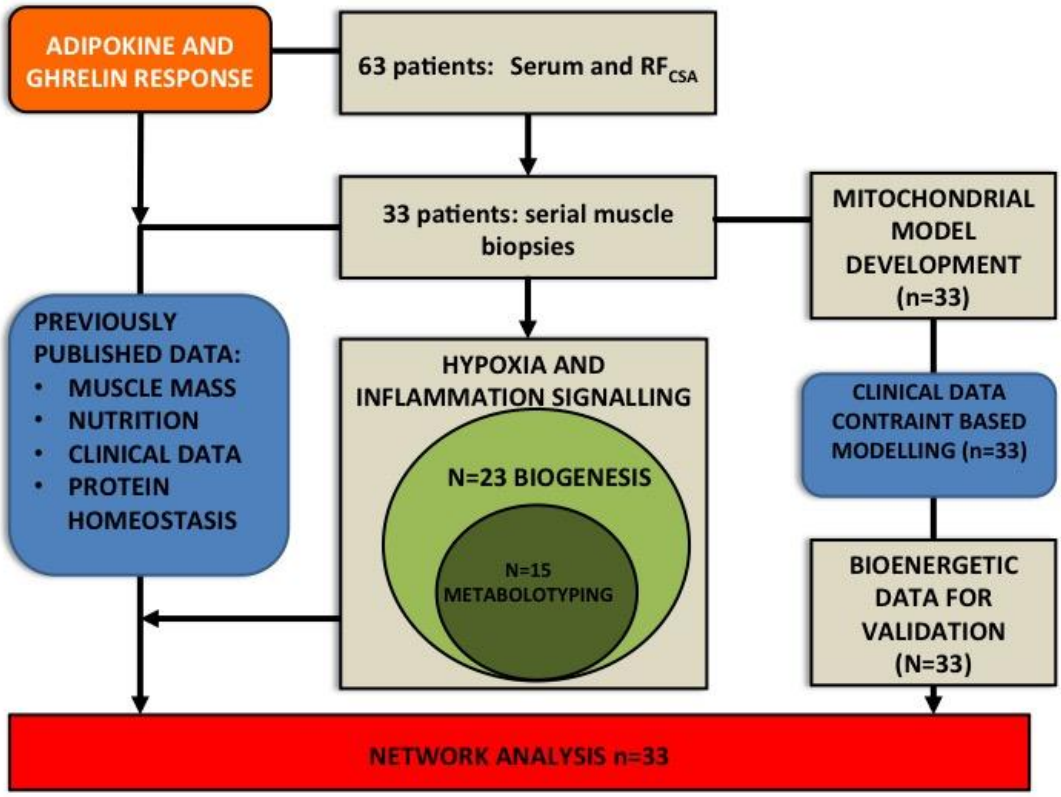

Figure S1: Consort flowchart of cohorts

2. Mitochondrial proteins

Median Florescence Index (MFI) for protein concentrations of mitochondrial respiratory chain complexes were normalised for NNT (a housekeeping protein used as part of the Luminex platform analysis).

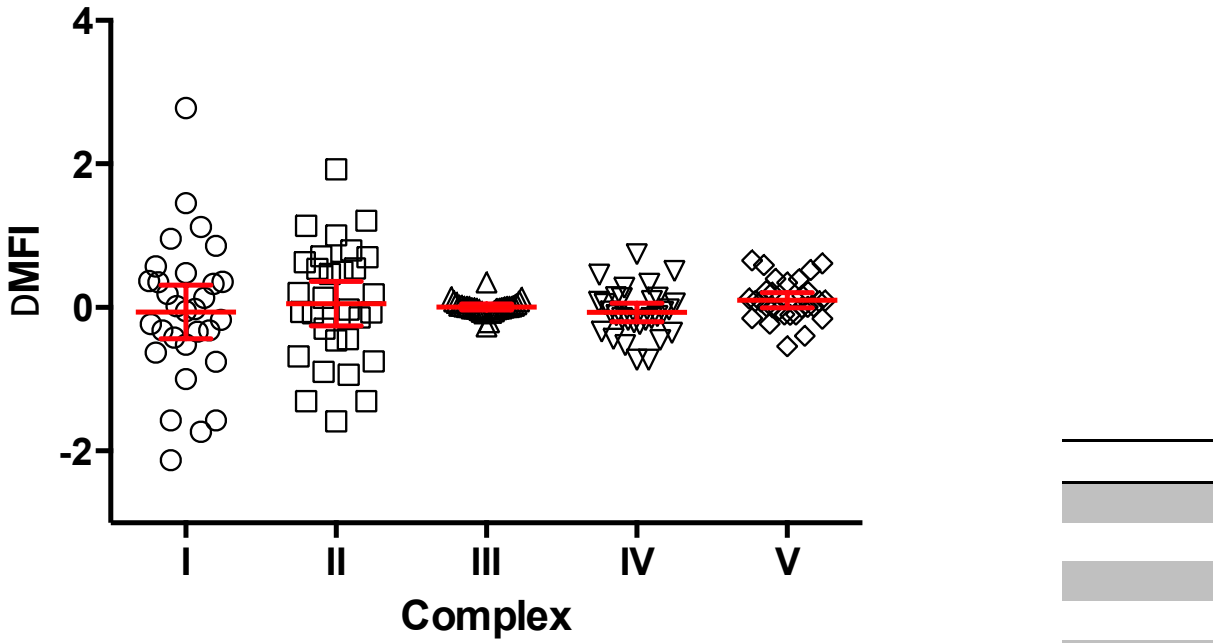

V	0.19 [0.11-0.26]	0.29 [0.18-0.40]	0.070

.

Figure S2 and Table S4: Change in intramuscular mitochondrial complex concentrations over 7 days of critical Illness (n=30), normalised to NNT (housekeeping protein). Data are mean and 95% Confidence Intervals. P values are for two-tailed Wilcoxon signed rank test. * denotes p<0.05. MFI= Median Florescence Index

2.Beta Oxidation Enzymes

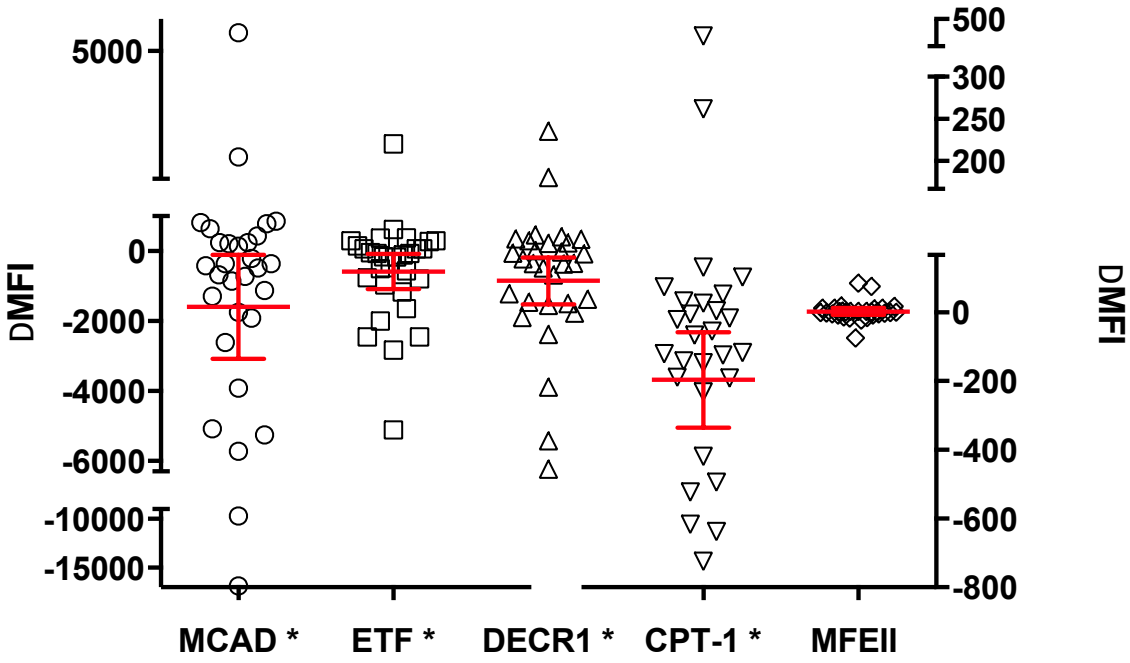

Beta-Oxidation	Day 1	Day 7	p
CPT-1	373 [219-528]	177 [69-284]	**0.006***
MCAD	2821 [1444-4198]	1233 [677-1790]	**0.028***
ETF	1159 [671.2-1647]	578 [316-840]	**0.046***
DECR1	1485 [786.1-2183]	639 [317-961]	**0.018***
MFEII	9.21 [3.7-14.7]	12.0 [4.5-19.5]	0.666

Figure S3 and Table S5: Change in intramuscular beta-oxidation enzyme concentrations over 7 days of critical illness. Data are mean and 95% Confidence Intervals. P values are for two-tailed Wilcoxon signed rank test, *denotes p<0.05. CPT= Carnitine palmitolytransferase I; MCAD= Medium Chain Acyl-Coenzyme A Dehydrogenase; ETF= Electron Transfer Flavoprotein; DECR1= 2,4, Dienoyl-CoA Reductase; MFEII= Multifunctional enzyme II. MFI= Median Florescence Index

3. Mitochondrial biogenesis markers

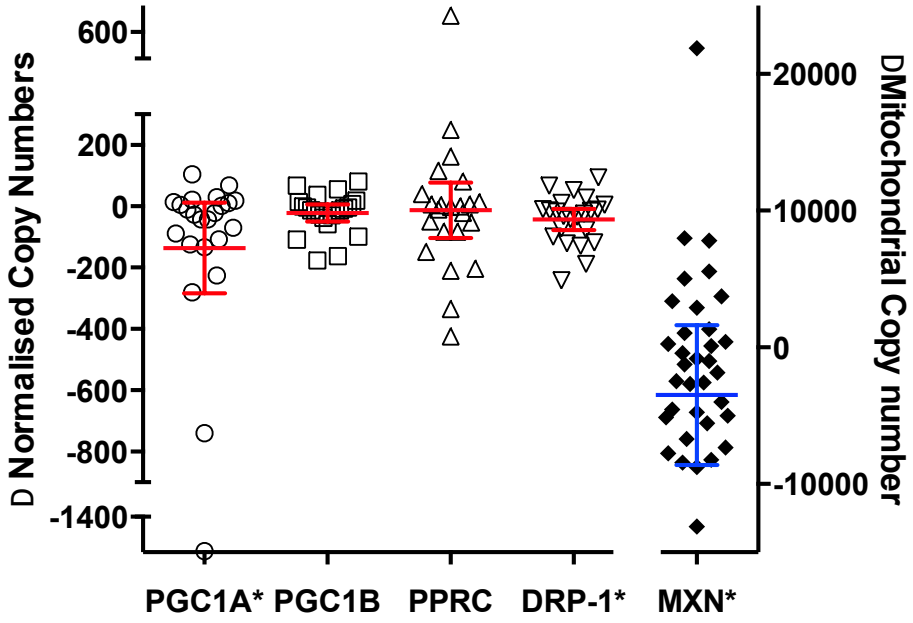

	Day 1	Day 7	p
PGC1α	206.3 [46.9-365.6]	69.8 [10.2-129.5]	**0.025***
PGC1β	68.6 [44.1-93.0]	46.7 [31.9-61.6]	0.132
PPRC	166.3 [110.6-222]	153.8 [90.6-217.1]	0.494
DRP-1	115.1 [84.2-146.0]	72.4 [56.0-88.8]	**0.018***
MXN	10388 [4958-15818]	6917 [4580-9254]	**0.032***

Figure S4 and Table S6: Change in intramuscular mitochondrial biogenesis markers over 7 days of critical illness. Data are normalised messenger Ribonucleic Acid copy number presented as mean and 95% Confidence Intervals. P values are for two-tailed Wilcoxon signed rank test. *denotes p<0.05. PGC1α= Peroxisome proliferator-activated receptor gamma co-activator 1-alpha; PGC1β= Peroxisome proliferator-activated receptor gamma co-activator 1-beta; PPRC= Peroxisome proliferator-activated receptor gamma co-activator; DRP-1= Dynamin Related Protein-1; MXN= Mitochondrial Copy Number

4. Bioenergetic Data

Table 6 delineates the breakdown of control subjects (n=41) of whom 48% had a chronic disease (compared to 46% of the patient cohort)). A wide age range was used in keeping with the critically ill cohort. No differences were seen between young (<30years) and older control subjects (all p>0.05) and between older controls and chronic disease patients (p>0.05). No relationship was seen between Oxygen Delivery (DO_2) and ATP content (n=9;r^2=0.29;p=0.133). No relationship was seen between ATP content on day 1 and admission PaO_2 (r^2=0.002, p=0.809; n=32), SaO_2 (r^2=0.00; p=0.973;n=32) or PaO_2 to FiO_2 ratio (r^2=0.006, p=0.684;n=32). Old controls were 77.8% male and weighed 76.1y±10.8kg (BMI 25.6±4.0), young controls were 100% male and weighed 74.5±2.2kg. All were healthy controls with no known co-morbidities"

	Young Controls	**Older controls**	**Stable COPD**
Age[#]	24±0.7	67.5±6.8	69±7.0
N	7	9	15
ATP (mmol/kg dw)	21.7 (20.4-22.9)	21.6 (18.8-24.3)	21.1 (19.0-23.2)
PCr (mmol/kg dw)	72.7 (69.0-76.4)	70.9 (65.2-76.6)	73.7 (66.9-80.4)
Total Creatine (mmol/kg dw)	126.0 (120.7-131.2)	121.3 (113.3-129.4)	129.2 (118.9-139.5)

Table S7: Bioenergetic data for control subjects. Data are mean (95%CI) except for # mean (SD). ATP= Adenosine Triphosphate, COPD=Chronic Obstructive Pulmonary Disease.

Variable	**Slope**	**95%CI**	**Intercept**	**R^2**	**P**
Insulin[#]	-0.996	-1.892—0.100	1.393	0.15	**0.031**
Glucose(blood)[#$]			1.000	0.09	0.097
Protein	-2.689	-6.153-0.774	6.968	0.08	0.123
Calories	-61.300	-152.30-29.71	190.0	0.06	0.179
Fat (total)	-2.960	-8.48-1.153	9.046	0.04	0.282
Saturated Fat[#]	-0.0183	-0.111-0.074	1.072	0.01	0.164

Carbohydrates	-7.352	-18.81-4.11	22.08	0.06	0.200
Polysaccharides	-1.534	-16.69-13.62	11.84	0.00	0.837
Glucose (feed)#	-0.052	-0.913-0.808	0.015	0.00	0.902

Table S8: relationship between nutritional delivery and bioenergetic data: Change in ATP was used as the dependent variable. # denotes log transformed data. Nutritional data units are g/kg/ibw.

5. *Metabotyping*

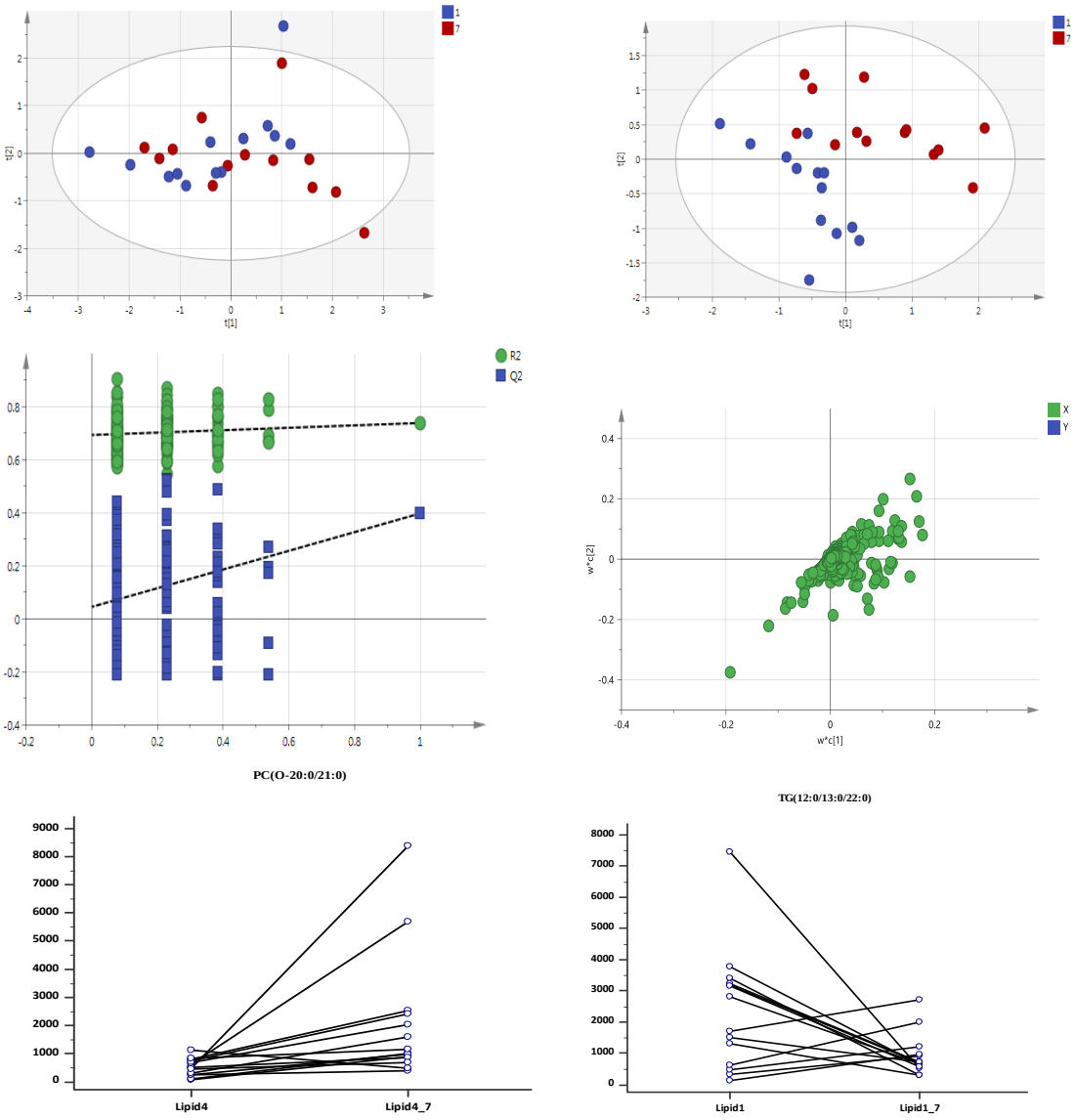

Figure S6 A) Principal Component analysis (PCA) of Ultra Performance liquid chromatography mass spectrometry data for muscle samples on day 1 and day 7 indicating poor initial discrimination (R2X=0.473, Q2Y=0.397) B PLSDA of the same sample set indicating visual discrimination and borderline multivariate model validity (RwX=0.338, R2Y=0.701, Q2Y=0.397 CV ANOVA p=0.021), C) Permutation analysis , D) Loadings plot of PLSDA mode, E) and F) dot and line diagrams of metabolites retaining significant a statistically significant difference in arbitrary concentration (all spectra normalised for weight of muscle used, p values E <0.01, F 0.02).

Using the marker table for adducts in the organic phase, multivariate analysis was performed. Using PLSDA and a 2-component model, it was possible to discriminate between the markers present in muscle samples on day 1 and day 7. This 2-component cross-validated model had an R^2Y of 0.72 and Q^2 of 0.41 and AUROC of 0.95 for predicting day of muscle sampling. The CV-ANOVA p-value of this model was 0.02 suggesting that this was valid, although permutation analysis demonstrated this model to be of borderline validity. The markers of greatest discrimination were mostly phospholipid moieties of varying point of saturation and chain length (PC 36:3, 36:4, 32:0, 41:0) and one triglyceride (side chains 12:0/13:0/22:0).

Variable	Slope	95%CI	Intercept	R^2	P
Medium Chain Triglycerides	0.003	-0.008-0.018	0.413	0.000	0.963
Monounsaturated FAs	0.001	-0.000-0.002	6.772	0.123	0.320
Polyunsaturated FAs	0.002	-0.003-0.009	14.420	0.141	0.286
Phospholipids	0.113	0.007-0.220	422.600	0.427	**0.041***
Saturated	0.001	-0.001-0.002	4.401	0.134	0.298

Table S9: Associations between change in intramuscular phosphocholine and nutritional delivery. over 7 days. Data are total amount delivered over 7 days normalised to ideal body weight expressed as mean (95%CI) units are mg/kg. FA= Fatty Acids. *denotes p<0.05.

6. AMPK Western Blots

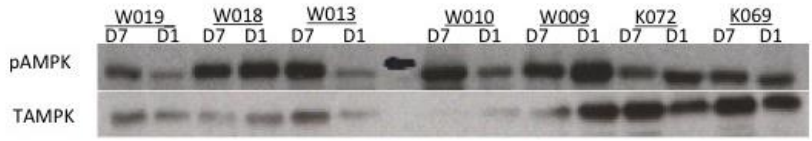

Figure S7: Western Blots of Phosphorylated (p-AMPK) and Total (TAMPK) Adenosine Monophosphate Kinase. W numbers are Unique identification numbers. D1 and D7 represent days from admission to Intensive care.

Neither total AMPK (1.28AU (95%CI 0.843-1.715) vs. 0.931AU (95%CI 0.588-1.276); p=0.0635) nor phosphorylated AMPK changed over 7 days (1.229AU (95%CI 0.880-1.58) vs. 1.255 AU (95%CI 1.06-1.45); p=0.692). However the ratio of phosphorylated to total AMP-K concentrations rose (1.06 (95%CI 0.82-1.30) to 3.93 (95%CI 1.30-6.56); n=31; p=0.001).

7. Adipokinin response

Adipokinin	Day 1	Day 3	Day 7	Day 10
Adiponectin	23.7 (19.2-28.1)	26.2 (21.6-30.9)	33.9 (28.6-39.3)*	36.5 (31.3-41.8)*
Resistin	4.1 (3.2-5.1)	4.1 (3.2-5.0)	3.5 (2.8-3.9)	3.5 (2.7-4.2)
Leptin #	10.5 (7.6-13.4)	10.9 (8.2-13.7)	10.1 (7.3-12.9)	10.1 (7.6-12.7)
Ghrelin#	105.9(57.5-	138.4 (75.2-	164.3 (83.72-	193.5 (102.7-

	154.4)	201.5)	244.9)*	284.2)*

Table S10: Serum Adipokinin response over first 10 days of critical illness (n=60). Data are mean (95%Confidence Intervals). * represent p<0.05 for Freidman's test (data are non-parametric). Units are microgram/ml except # indicating nanograms/ml.

7.1 Longitudinal changes in Leptin by sex and obese/non obese

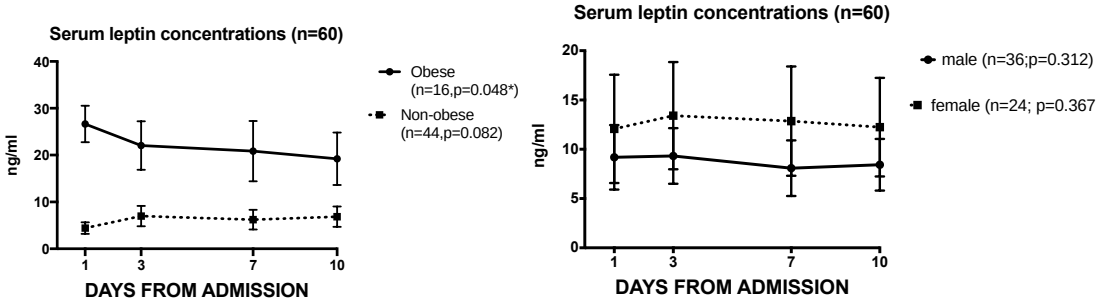

Figure S8AB: Longitudinal change in Leptin by obesity (left panel) and sex (right panel) over 10 days of critical illness (n=60). Data are mean (95%Confidence Intervals). *represent p<0.05 for Freidman's test (data are non-parametric).

9. Hypoxia inducible factor associations

The change in intramuscular phosphocholine was not related to change in intramuscular HIF1α signaling (r^2=0.35; p=0.068), nor was change in intramuscular triglyceride (r^2=0.08;p=0.408).

Value	Slope	95%CI	Intercept	R^2	P value
ΔPaO_2	-0.159	-0.046-0.014	-0.553	-0.052	0.283
ΔSaO_2	-0.041	-0.113-0.195	-5.269	-0.011	0.588
ΔP/F ratio	-0.019	-0.133-0.096	6.747	0.003	0.739

Table S11: Bivariable linear regression with change in Hypoxia inducible Factor 1 alpha as the dependent variable. PaO_2= Partial Pressure of Arterial Oxygen, SAO_2=Saturation of Arterial Oxygen, P/F ratio= ratio of PaO_2 to Fraction of inspired oxygen.

Variable	Slope	95%CI	Intercept	R^2	P
Il-1α	0.003	-0.031- 0.037	0.142	0.001	0.862
Il-1β	-0.244	-0.877- 0.389	24.160	0.022	0.436
Il-2	-0.201	-0.677- 0.269	-3.863	0.027	0.389
Il-4	-0.043	-4.377- 4.291	220.200	0.000	0.984
Il-6	0.959	-0.108- 2.026	-2.531	0.108	0.076
Il-8	23.570	10.770- 36.370	-85.620	0.337	**0.001***
Il-10	-0.347	-0.949- 0.259	44.340	0.047	0.248

TNF-α	-0.710	-3.317- 1.897	64.150	0.011	0.581
INFγ	-0.014	-0.132- 0.104	1.037	0.002	0.811
MCP1	6.562	1.668- 11.460	-45.130	0.212	**0.010***
EGF	-0.122	-0.471- 0.226	3.229	0.018	0.478
TNFR1	0.027	0.007- 0.047	0.585	0.192	**0.011***
TNFR2	0.026	-0.010- 0.062	-0.133	0.065	0.153

Table 12: Bivariable linear regression with change in Hypoxia inducible Factor 1 alpha as the dependent variable. TNFα= Tumour Necrosis Factor Alpha; IFN- γ= Interferon gamma; EGF= Epithelial Growth Factor; Il=Interleukin; MCP-1= Macrophage Chemotactic Protein-1; TNFR= Tumour Necrosis Factor Receptor

10. Lipids delivered as components of nutrition or sedation (n=33) entered into Network analysis

mg/kg	Nutrition	Propofol
Saturated	**1.1 (0.9-1.2)**	**2.3 (1.5-3.1)**
Medium Chain Triglycerides	**0.6 (0.5-0.7)**	**0 (0.0-0.0)**
Polyunsaturated	**1.0 (0.7-1.4)**	**8.8 (5.6-11.9)**
Monounsaturated	**2.3 (1.9-2.6)**	**3.3 (2.1-4.4)**
Phospholipids	**34 (-7-75.7)**	**171.9 (110-234)**

Table S13: Data are total amount delivered over 7 days normalised to ideal body weight expressed as mean (95%CI) units are mg/kg

Variable	Slope	95%CI	Intercept	R^2	P
Medium Chain Triglycerides	0.001	0.000-0.002	0.577	0.153	**0.027***
Monounsaturated FAs	0.001	-0.011-0.013	5.598	0.001	0.852
Polyunsaturated FAs	-0.006	-0.035-0.0224	9.984	0.006	0.667
Phospholipids	-0.211	-0.845-0.424	210.500	0.015	0.503
Saturated Fats	0.000	-0.008-0.008	3.417	0.000	0.986
Polysaccharides	0.010	-0.010-0.030	10.740	0.038	0.321

Table S14: Associations between nutritional delivery and change in serum C-Reactive Protein concentration over 7 days. Data are total amount delivered over 7 days normalised to ideal body weight expressed as mean (95%CI) units are mg/kg. FA= Fatty Acids. *denotes p<0.05.

11. Network analysis and interactions

Network prior to Data Clustering

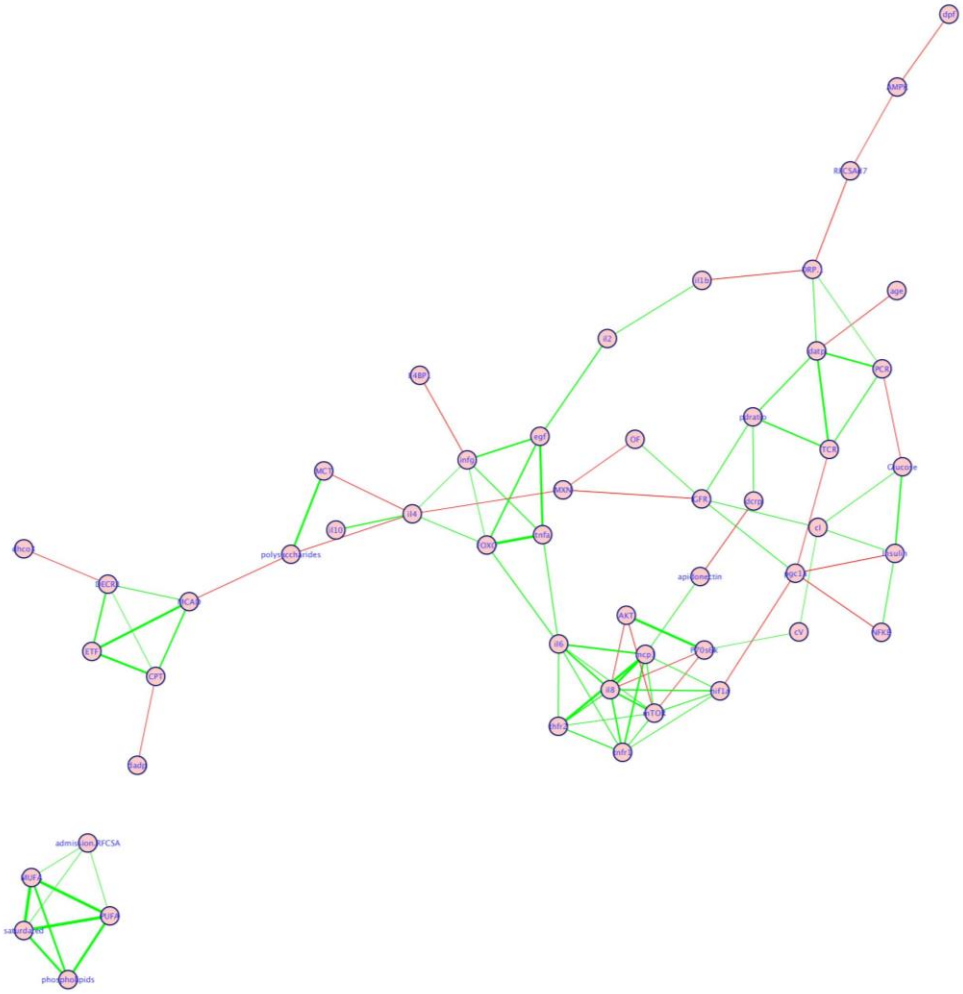

Figure S10: Network analysis prior to Cluster analysis. Green lines represent positive correlations, red lines negative.

Data Clusters

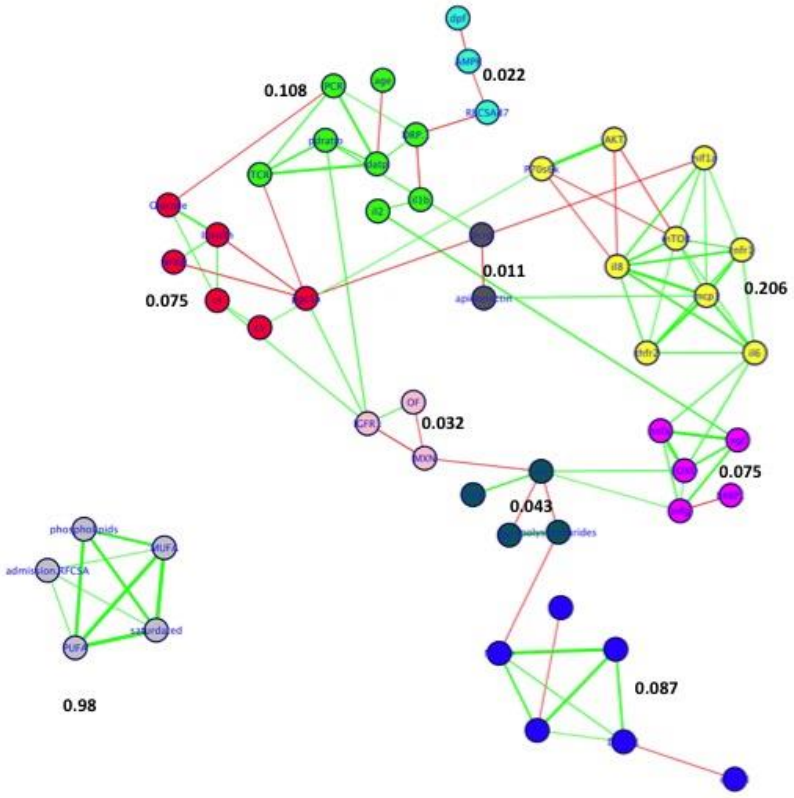

Figure S11: Markov Clusters of the multi-dimensional network. Colours represent actual clusters as opposed to data types. Values modularity calculations for each cluster.

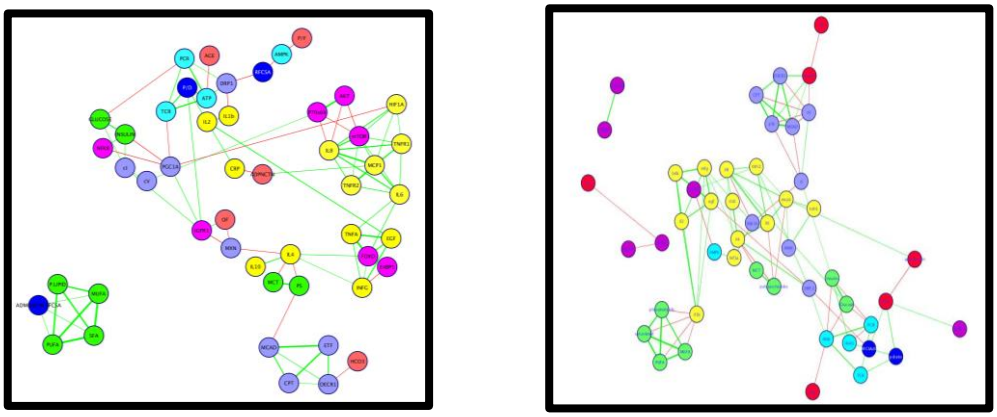

Figure s12: Network analysis using Pearson correlation (left panel) and Spearman correlation (Right panel) demonstrating similar cluster delineation.

Analysis of Interactions

NODE	INTERACTION	NODE	INTERACTION
CLUSTER 1+2			
P/D ratio <--> ATP[9]	0.534	ATP <--> PCR[10]	0.687
P/D ratio <--> TCR[9 11]	0.625	ATP <--> TCR[10]	0.730
DRP-1 <--> ATP[12 13]	0.465	ATP <--> age[14]	-0.490
DRP-1 <--> PCR[12 13]	0.405	DRP-1 <--> RF_{CSA}[15]	-0.551
PCR <--> TCR[10 11]	0.516	AMPK <--> RF_{CSA}[16]	-0.405
AMPK <--> P/F ratio[17]	-0.496	Il-1β <--> DRP-1[18]	-0.562
Il-1β <--> Il-2[19]	0.451		
CLUSTER 3			
PGC1α <--> TCR[20 21]	-0.440	cV <--> cI[22]	0.405
PGC1α <--> NFKβ[23]	-0.713	NFKβ <--> Insulin[24]	0.475
Glucose <--> Insulin[25]	0.626	cI <--> Glucose[26]	0.429
PGC1α <--> Insulin[20 21]	-0.754	cI <--> Insulin[26]	0.441
CLUSTER 4			
P70s6k <--> AKT[8]	0.865	Il-6 <--> Il-8[27]	0.663
P70s6k <--> mTOR[8]	-0.434	Il-6 <--> MCP-1[28]	0.681
AKT <--> mTOR[8 29]	-0.571	Il-6 <--> TNFR1[30]	0.490
Il-8 <--> MCP-1[31]	0.820	Il-6 <--> TNFR2[19 30]	0.504
Il-8 <--> TNFR1[32]	0.655	Il-6 <--> mTOR[33 34]	0.452
Il-8 <--> TNFR2[32]	0.537	MCP-1 <--> TNFR1[35]	0.675
Il-8 <--> HIF1α [36]	0.581	MCP-1 <--> TNFR2[37]	0.846
Il-8 <--> P70s6k[32]	-0.461	MCP-1 <--> HIF1α[38]	0.461
Il-8 <--> AKT[32]	-0.506	TNFR1 <--> TNFR2[30]	0.543
Il-8 <--> mTOR[32]	0.673	TNFR1 <--> HIF1 α[36]	0.438
MCP-1 <--> mTOR[31]	0.496	TNFR1 <--> mTOR[30]	0.483
HIF1α <--> mTOR[39]	0.484	TNFR2 <--> mTOR[33]	0.435
CLUSTER 5			
TNFα <--> INFγ[40]	0.511	EGF<--> FOXO-1[41]	0.632
TNFα <--> EGF[42]	0.790	INFγ <--> EGF[43]	0.650
TNFα <--> FOXO-1[33]	0.903	INFγ <--> FOXO-1[44]	0.418
		INFγ<--> E4BP1[45]	-0.537
CLUSTER 6			
MCAD <--> PS[46]	-0.468	DECR1 <--> HCO_3[47]	-0.416
CPT-1 <--> MCAD[48]	0.627	CPT-1 <--> ETF[48]	0.794
MCAD <--> ETF[48]	0.832	CPT-1<--> DECR1[48]	0.403
MCAD <--> DECR1[48]	0.458	ETF <--> DECR1[48]	0.650
CLUSTER 7			
PUFA <--> PL[49-52]	0.863	PUFA <--> sFA[49-51]	0.984
MUFA <--> Day 1.RF_{CSA}[53 54]	0.402	MUFA <--> PUFA[49-51]	0.958
PUFA <--> Day1.RF_{CSA}[53 54]	0.414	MUFA <--> PL[49-52]	0.750

MUFA <--> sFA[49-51]	0.991	PL <--> sFA[49-52]	0.803
sFA <--> Day1.RF_{CSA}[53 54]	0.411		
CLUSTERS 8 and 9			
MXN <--> IGFR1[55]	-0.827	MXN <--> OF[20 56]	-0.400
IGFR1 <--> OF[8]	0.434	MCT <--> PS[49-51]	0.750
Il-4 <--> FOXO-1[57]	0.451	Il-4 <--> Il-10[58]	0.562
Il-4 <--> MCT[59]	-0.485	Il-4 <--> INFγ[58]	0.402
Il-4 <-->PS[60]	-0.475	Il-4 <--> MXN[61]	-0.435
INTER-CLUSTER INTERACTIONS			
PGC1α <--> IGFR1[55]	0.461	Il-6 <--> TNFα[19]	0.491
hif1α <--> PGC1α[62]	-0.510	Il-6 <--> FOXO-1[63]	0.518
P/D ratio <--> IGFR1[8]	0.485	P/D ratio <--> CRP[8]	0.480
IGFR1 <--> cI[64]	0.448	PCR <--> Glucose[11 65]	-0.447
MCP-1 <--> apidonectin[28]	0.456	P70s6k <--> cV[64]	0.402
apidonectin <--> CRP[28]	-0.543		

Table S15: Heatmap detailing biological plausibility of interactions seen in network analysis. Heatmap key is seen below. P/D ratio= Protein:DNA ratio; ATP= Adenosine Tri-Phosphate; RF_{CSA}= Rectus Femoris Cross Sectional Area, PGC1α= Peroxisome Proliferator-activated Receptor gamma co-activator 1 alpha; DRP-1= Dynamin Related Protein 1; MXN= Mitochondrial Copy Number; HIF1α= Hypoxia Inducible Factor 1 alpha; TNFα= Tumour Necrosis Factor Alpha; IFN- γ= Interferon gamma; EGF= Epithelial Growth Factor; Il=Interleukin; MCP-1= Macrophage Chemotactic Protein-1; AMP-K=Adenosine Mono Phosphate Kinase; ATP= Adenosine Triphosphate; CR= Creatine; PCR= Phosphocreatine; CPT-1= Carnitine Palmitoyltransferase-1; MCAD= Medium Chain Acyl-CoA Dehydrogenase; ETF= electron Transferring Flavoprotein; DECR1= 2,4-dienoyl-CoA reductase 1; MFEII= Multifunctional Enzyme-2; NFKB= Nuclear Factor Kappa Beta; IGFR1=Insulin-like Growth Factor 1; cV=Complex V; P70s6K= Ribosmal protein S6 Kinase; FOXO-1= Forkhead Group O-1; mTOR= Mammalian Target of Rapamycin; AKt= Protein Kinase B; E4BP1= Eukaryotic translation initiation factor 4E-binding protein 1; PUFA=Polyunsaturated Fatty Acids; MUFA=Monounsaturated Fatty Acids; SFA= Saturated Fatty Acids; PS= Polysaccharides; PL= phospholipids.

	ANIMALS		HUMAN TISSUE	
NO DATA	Plausible	Demonstrated	Plausible	Demonstrated

REFERENCES

1. Malik AN, Shahni R, Rodriguez-de-Ledesma A, et al. Mitochondrial DNA as a non-invasive biomarker: accurate quantification using real time quantitative PCR without co-amplification of pseudogenes and dilution bias. Biochem Biophys Res Commun 2011;**412**(1):1-7.
2. Anwar MA, Vorkas PA, Li JV, et al. Optimization of metabolite extraction of human vein tissue for ultra performance liquid chromatography-mass spectrometry and nuclear magnetic resonance-based untargeted metabolic profiling. Analyst 2015;**140**(22):7586-97.
3. Vorkas PA, Isaac G, Anwar MA, et al. Untargeted UPLC-MS profiling pipeline to expand tissue metabolome coverage: application to cardiovascular disease. Anal Chem 2015;**87**(8):4184-93.
4. Jakobsson P, Jorfeldt L, Brundin A. Skeletal muscle metabolites and fibre types in patients with advanced chronic obstructive pulmonary disease (COPD),

with and without chronic respiratory failure. Eur Respir J 1990;**3**(2):192-6.
5. Steiner MC, Evans R, Deacon SJ, et al. Adenine nucleotide loss in the skeletal muscles during exercise in chronic obstructive pulmonary disease. Thorax 2005;**60**(11):932-6.
6. van Loon LJ, Greenhaff PL, Constantin-Teodosiu D, et al. The effects of increasing exercise intensity on muscle fuel utilisation in humans. The Journal of physiology 2001;**536**(Pt 1):295-304.
7. Constantin-Teodosiu D, Constantin D, Stephens F, et al. The role of FOXO and PPAR transcription factors in diet-mediated inhibition of PDC activation and carbohydrate oxidation during exercise in humans and the role of pharmacological activation of PDC in overriding these changes. Diabetes 2012;**61**(5):1017-24.
8. Puthucheary ZA, Rawal J, McPhail M, et al. Acute skeletal muscle wasting in critical illness. JAMA 2013;**310**(15):1591-600.
9. Research IoMUCoMN. The Energy Costs of Protein Metabolism: Lean and Mean on Uncle Sam's Team. The Role of Protein and Amino Acids in Sustaining and Enhancing Performance. Washington (DC): National Academies Press (US), 1999.
10. Wyss M, Kaddurah-Daouk R. Creatine and creatinine metabolism. Physiol Rev 2000;**80**(3):1107-213.
11. Cooper R, Naclerio F, Allgrove J, et al. Creatine supplementation with specific view to exercise/sports performance: an update. J Int Soc Sports Nutr 2012;**9**(1):33.
12. Shields LY, Kim H, Zhu L, et al. Dynamin-related protein 1 is required for normal mitochondrial bioenergetic and synaptic function in CA1 hippocampal neurons. Cell Death Dis 2015;**6**:e1725.
13. Reddy PH, Reddy TP, Manczak M, et al. Dynamin-related protein 1 and mitochondrial fragmentation in neurodegenerative diseases. Brain Res Rev 2011;**67**(1-2):103-18.
14. Shigenaga MK, Hagen TM, Ames BN. Oxidative damage and mitochondrial decay in aging. Proceedings of the National Academy of Sciences of the United States of America 1994;**91**(23):10771-8.
15. Deng H, Dodson MW, Huang H, et al. The Parkinson's disease genes pink1 and parkin promote mitochondrial fission and/or inhibit fusion in Drosophila. Proceedings of the National Academy of Sciences of the United States of America 2008;**105**(38):14503-8.
16. Gordon SE, Lake JA, Westerkamp CM, et al. Does AMP-activated protein kinase negatively mediate aged fast-twitch skeletal muscle mass? Exerc Sport Sci Rev 2008;**36**(4):179-86.
17. Zhao X, Zmijewski JW, Lorne E, et al. Activation of AMPK attenuates neutrophil proinflammatory activity and decreases the severity of acute lung injury. Am J Physiol Lung Cell Mol Physiol 2008;**295**(3):L497-504.
18. Roth D, Krammer PH, Gulow K. Dynamin related protein 1-dependent mitochondrial fission regulates oxidative signalling in T cells. FEBS Lett 2014;**588**(9):1749-54.
19. Delgado AV, McManus AT, Chambers JP. Production of tumor necrosis factor-alpha, interleukin 1-beta, interleukin 2, and interleukin 6 by rat leukocyte

subpopulations after exposure to substance P. Neuropeptides 2003;**37**(6):355-61.
20. Carre JE, Orban JC, Re L, et al. Survival in critical illness is associated with early activation of mitochondrial biogenesis. American journal of respiratory and critical care medicine 2010;**182**(6):745-51.
21. Crouser ED. Peroxisome Proliferator-Activated Receptors {gamma} Coactivator-1{alpha}: Master Regulator of Mitochondrial Biogenesis and Survival during Critical Illness? Am J Respir Crit Care Med 2010;**182**(6):726-28.
22. Kuhlbrandt W. Structure and function of mitochondrial membrane protein complexes. BMC Biol 2015;**13**:89.
23. Yang XY, Wang LH, Mihalic K, et al. Interleukin (IL)-4 indirectly suppresses IL-2 production by human T lymphocytes via peroxisome proliferator-activated receptor gamma activated by macrophage-derived 12/15-lipoxygenase ligands. J Biol Chem 2002;**277**(6):3973-8.
24. Kim F, Pham M, Luttrell I, et al. Toll-like receptor-4 mediates vascular inflammation and insulin resistance in diet-induced obesity. Circ Res 2007;**100**(11):1589-96.
25. Saltiel AR, Kahn CR. Insulin signalling and the regulation of glucose and lipid metabolism. Nature 2001;**414**(6865):799-806.
26. Asmann YW, Stump CS, Short KR, et al. Skeletal muscle mitochondrial functions, mitochondrial DNA copy numbers, and gene transcript profiles in type 2 diabetic and nondiabetic subjects at equal levels of low or high insulin and euglycemia. Diabetes 2006;**55**(12):3309-19.
27. Hooper WC, Phillips DJ, Renshaw MA, et al. The up-regulation of IL-6 and IL-8 in human endothelial cells by activated protein C. J Immunol 1998;**161**(5):2567-73.
28. Zoico E, Garbin U, Olioso D, et al. The effects of adiponectin on interleukin-6 and MCP-1 secretion in lipopolysaccharide-treated 3T3-L1 adipocytes: role of the NF-kappaB pathway. Int J Mol Med 2009;**24**(6):847-51.
29. Hay N, Sonenberg N. Upstream and downstream of mTOR. Genes Dev 2004;**18**(16):1926-45.
30. Schulz R, Heusch G. Tumor necrosis factor-alpha and its receptors 1 and 2: Yin and Yang in myocardial infarction? Circulation 2009;**119**(10):1355-7.
31. Lin HY, Chang KT, Hung CC, et al. Effects of the mTOR inhibitor rapamycin on monocyte-secreted chemokines. BMC Immunol 2014;**15**:37.
32. Osawa Y, Nagaki M, Banno Y, et al. Tumor necrosis factor alpha-induced interleukin-8 production via NF-kappaB and phosphatidylinositol 3-kinase/Akt pathways inhibits cell apoptosis in human hepatocytes. Infect Immun 2002;**70**(11):6294-301.
33. Constantin D, McCullough J, Mahajan RP, et al. Novel events in the molecular regulation of muscle mass in critically ill patients. The Journal of physiology 2011;**589**(Pt 15):3883-95.
34. Crossland H, Constantin-Teodosiu D, Gardiner SM, et al. A potential role for Akt/FOXO signalling in both protein loss and the impairment of muscle carbohydrate oxidation during sepsis in rodent skeletal muscle. The Journal of physiology 2008;**586**(Pt 22):5589-600.
35. Barna BP, Pettay J, Barnett GH, et al. Regulation of monocyte chemoattractant protein-1 expression in adult human non-neoplastic astrocytes is

sensitive to tumor necrosis factor (TNF) or antibody to the 55-kDa TNF receptor. J Neuroimmunol 1994;**50**(1):101-7.
36. Bartels K, Grenz A, Eltzschig HK. Hypoxia and inflammation are two sides of the same coin. Proceedings of the National Academy of Sciences of the United States of America 2013;**110**(46):18351-2.
37. Johrer K, Janke K, Krugmann J, et al. Transendothelial migration of myeloma cells is increased by tumor necrosis factor (TNF)-alpha via TNF receptor 2 and autocrine up-regulation of MCP-1. Clin Cancer Res 2004;**10**(6):1901-10.
38. Mojsilovic-Petrovic J, Callaghan D, Cui H, et al. Hypoxia-inducible factor-1 (HIF-1) is involved in the regulation of hypoxia-stimulated expression of monocyte chemoattractant protein-1 (MCP-1/CCL2) and MCP-5 (Ccl12) in astrocytes. J Neuroinflammation 2007;**4**:12.
39. Etheridge T, Atherton PJ, Wilkinson D, et al. Effects of hypoxia on muscle protein synthesis and anabolic signaling at rest and in response to acute resistance exercise. Am J Physiol Endocrinol Metab 2011;**301**(4):E697-702.
40. D'Andrea A, Aste-Amezaga M, Valiante NM, et al. Interleukin 10 (IL-10) inhibits human lymphocyte interferon gamma-production by suppressing natural killer cell stimulatory factor/IL-12 synthesis in accessory cells. J Exp Med 1993;**178**(3):1041-8.
41. Jackson JG, Kreisberg JI, Koterba AP, et al. Phosphorylation and nuclear exclusion of the forkhead transcription factor FKHR after epidermal growth factor treatment in human breast cancer cells. Oncogene 2000;**19**(40):4574-81.
42. Akca H, Akan SY, Yanikoglu A, et al. Suppression of TNF-alpha mediated apoptosis by EGF in TNF-alpha sensitive human cervical carcinoma cell line. Growth Factors 2003;**21**(1):31-9.
43. Worm M, Makki A, Dippel E, et al. Interferon-gamma downregulates epidermal growth factor receptors on human melanoma cells. Exp Dermatol 1995;**4**(1):30-5.
44. Li P, Zhao Y, Wu X, et al. Interferon gamma (IFN-gamma) disrupts energy expenditure and metabolic homeostasis by suppressing SIRT1 transcription. Nucleic Acids Res 2012;**40**(4):1609-20.
45. Li P, Du Q, Cao Z, et al. Interferon-gamma induces autophagy with growth inhibition and cell death in human hepatocellular carcinoma (HCC) cells through interferon-regulatory factor-1 (IRF-1). Cancer Lett 2012;**314**(2):213-22.
46. Gross DN, van den Heuvel AP, Birnbaum MJ. The role of FoxO in the regulation of metabolism. Oncogene 2008;**27**(16):2320-36.
47. Kompare M, Rizzo WB. Mitochondrial fatty-acid oxidation disorders. Semin Pediatr Neurol 2008;**15**(3):140-9.
48. Houten SM, Wanders RJ. A general introduction to the biochemistry of mitochondrial fatty acid beta-oxidation. Journal of inherited metabolic disease 2010;**33**(5):469-77.
49. Nutricia. Oral nutritional supplements. Secondary Oral nutritional supplements 2015. http://nutricia.co.uk/files/uploads/documents/Nutricia_ONS_Product_Compendium.pdf.

50. Kabiven. Secondary 2014. http://www.kabivenusa.com/pdf/Kabiven_PI.pdf.
51. Nutrition A. Secondary. https://www.abbottnutrition.co.uk/products-and-services/Abbott-Nutrition-Products/jevity-plus.
52. Formulary BN. Propofol. Secondary Propofol 2016. http://www.evidence.nhs.uk/formulary/bnf/current/15-anaesthesia/151-general-anaesthesia/1511-intravenous-anaesthetics/drugs-used-for-intravenous-anaesthesia/propofol.
53. Kreymann KG, Berger MM, Deutz NE, et al. ESPEN Guidelines on Enteral Nutrition: Intensive care. Clin Nutr 2006;**25**(2):210-23.
54. McClave SA, Taylor BE, Martindale RG, et al. Guidelines for the Provision and Assessment of Nutrition Support Therapy in the Adult Critically Ill Patient: Society of Critical Care Medicine (SCCM) and American Society for Parenteral and Enteral Nutrition (A.S.P.E.N.). J Parenter Enteral Nutr 2016;**40**(2):159-211.
55. Ibebunjo C, Eash JK, Li C, et al. Voluntary running, skeletal muscle gene expression, and signaling inversely regulated by orchidectomy and testosterone replacement. Am J Physiol Endocrinol Metab 2011;**300**(2):E327-40.
56. Brealey D, Brand M, Hargreaves I, et al. Association between mitochondrial dysfunction and severity and outcome of septic shock. Lancet 2002;**360**(9328):219-23.
57. Luzina IG, Keegan AD, Heller NM, et al. Regulation of inflammation by interleukin-4: a review of "alternatives". J Leukoc Biol 2012;**92**(4):753-64.
58. Luzina IG, Lockatell V, Lavania S, et al. Natural production and functional effects of alternatively spliced interleukin-4 protein in asthma. Cytokine 2012;**58**(1):20-6.
59. Prieur X, Mok CY, Velagapudi VR, et al. Differential lipid partitioning between adipocytes and tissue macrophages modulates macrophage lipotoxicity and M2/M1 polarization in obese mice. Diabetes 2011;**60**(3):797-809.
60. Kirmaz C, Bayrak P, Yilmaz O, et al. Effects of glucan treatment on the Th1/Th2 balance in patients with allergic rhinitis: a double-blind placebo-controlled study. European cytokine network 2005;**16**(2):128-34.
61. Kaminski MM, Sauer SW, Klemke CD, et al. Mitochondrial reactive oxygen species control T cell activation by regulating IL-2 and IL-4 expression: mechanism of ciprofloxacin-mediated immunosuppression. J Immunol 2010;**184**(9):4827-41.
62. O'Hagan KA, Cocchiglia S, Zhdanov AV, et al. PGC-1alpha is coupled to HIF-1alpha-dependent gene expression by increasing mitochondrial oxygen consumption in skeletal muscle cells. Proceedings of the National Academy of Sciences of the United States of America 2009;**106**(7):2188-93.
63. Ito Y, Daitoku H, Fukamizu A. Foxo1 increases pro-inflammatory gene expression by inducing C/EBPbeta in TNF-alpha-treated adipocytes. Biochem Biophys Res Commun 2009;**378**(2):290-5.
64. Guha M, Fang JK, Monks R, et al. Activation of Akt is essential for the propagation of mitochondrial respiratory stress signaling and activation of the transcriptional coactivator heterogeneous ribonucleoprotein A2. Mol Biol Cell 2010;**21**(20):3578-89.

65. Deldicque L, Atherton P, Patel R, et al. Effects of resistance exercise with and without creatine supplementation on gene expression and cell signaling in human skeletal muscle. J Appl Physiol (1985) 2008;**104**(2):371-8.